Electrochimica Acta 211 (2016) 998–1005

Contents lists available at ScienceDirect

Electrochimica Acta

journal homepage: www.elsevier.com/locate/electacta

Functionalized porous Si nanowires for selective and simultaneous electrochemical detection of Cd(II) and Pb(II) ions

Zheng Guo[a,b,*], Myeong-Lok Seol[b], Chao Gao[a], Moon-Seok Kim[b], Jae-Hyuk Ahn[b], Yang-Kyu Choi[b,**], Xing-Jiu Huang[a,**]

[a] Nanomaterials and Environmental Detection Laboratory, Institute of Intelligent Machines, Chinese Academy of Sciences, Hefei, 230031, PR China
[b] School of Electrical Engineering, Korea Advanced Institute of Science and Technology, 291 Daehak-ro, Yuseong-gu, Daejeon 34141, Republic of Korea

ARTICLE INFO

Article history:
Received 27 April 2016
Received in revised form 23 June 2016
Accepted 27 June 2016
Available online 27 June 2016

Keywords:
Porous
electrochemical detection
Si nanowires
heavy metal ions

ABSTRACT

Thiol and amino-functionalized porous Si nanowires have been demonstrated to selectively detect Cd(II) and Pb(II) with high sensitivity using square wave anodic stripping voltammetry (SWASV) analysis. Through a typical Ag-assisted chemical etching approach, uniform and porous Si nanowires have been fabricated on heavily doped Si wafer. Continuously functionalized by (3-mercaptopropyl)trimethoxysilane (MPTMS) and (3-aminopropyl)triethoxysilane (APTES), the internal and external surfaces of porous Si nanowires have been decorated with thiol and amino groups, respectively. Inspired by the intrinsic properties of porous nanostructures, their electrochemical performances toward heavy metal ions have been further evaluated. The results indicate that Cd(II) and Pb(II) can be detected with high sensitivity owing to the strong complexing capacity of thiol and amino groups. Additionally, porous Si nanowires decorated with thiol groups present different stripping behaviors from those with amino groups toward the investigated heavy metal ions, realizing the selective and simultaneous detection of Cd (II) and Pb(II). Furthermore, simultaneous detection of Cd(II) and Pb(II) has also been demonstrated without any interference and their individual high sensitivity has been fundamentally preserved. Expectedly, porous Si nanowires as an effective modifier can be further extended to selectively detect other heavy metal ions through modifying with other functional organic groups.

1. Introduction

Heavy metal ions, as one class of the most dangerous water pollutants, have been receiving great attention because they are extremely harmful in the biosphere and detrimental to human health [1–4]. Therefore, it is very important to get their specific information in the drinking water. Among various developed approaches, electrochemical analysis, especially for the anodic stripping voltammetry method as a powerful technique, has been widely employed to detect trace amount of various toxic metal ions due to its excellent sensitivity, short analysis time, portability and low cost, etc [5–10].

Undoubtedly, the sensitivity for anodic stripping voltammetry depends on the accumulation of the target metal ions [11,12]. Therefore, it is closely related to the modifiers of electrochemical electrode. Recently, nanomaterials have been extensively employed as promising modifiers owing to their large surface area and high adsorbing ability, which mainly focuses on carbon-based nanomaterials and metal oxide nanostructures [13–16]. Furthermore, the introduction of functional groups onto the modified electrode is also extremely attractive to obtain a selective determination of specific heavy metal ion [17–20]. However, for the modifiers of nanostructured metal oxides, their limitations mainly lie in the weak chemical stability that they can be etched in the acidic supporting electrolytes. For carbon-based nanomaterials (carbon nanotubes and graphene, etc), the required chemical modification is complex because of the removal of metal catalysts and their weak dispersion. In addition, their native structures are easily broken during the process of chemical modification. Hence, it still remains desirable and necessary to develop suitable nanomaterials as modifiers of electrochemical electrodes.

* Corresponding author at: Nanomaterials and Environmental Detection Laboratory, Institute of Intelligent Machines, Chinese Academy of Sciences, Hefei, 230031, PR China.
** Corresponding authors.
E-mail addresses: zhguo@iim.ac.cn (Z. Guo), ykchoi@ee.kaist.ac.kr (Y.-K. Choi), xingjiuhuang@iim.ac.cn (X.-J. Huang).

http://dx.doi.org/10.1016/j.electacta.2016.06.141
0013-4686/

Besides its famous electronic functionality, recently functional Si-based nanomaterials with meso-porous structures have been used to absorb heavy metal ions, motivated by their higher active surface-to-volume ratios in contrast to solid nanomaterials. Till now many functionalized porous silicas have been synthesized and successfully employed as adsorbents to remove heavy metal ions from wastewater [21–25]. Our previous reports have demonstrated that nanomaterials with selective absorption present selectively electrochemical response toward heavy metal ions. Following this view, Si nanomaterials should be expectedly applied as an alternative modifier to detect heavy metal ions. Superior to aforementioned carbon-based and metal oxide nanomaterials, Si nanomaterials are easily functionalized and with a good chemical stability. Actually, they have been employed as an advanced substrate and conducting pathways for constructing electrochemical sensors [26–28]. However, there are still few reports about the electrochemical detection of heavy metal ions using Si-based nanomaterials [29–32].

Inspired by their chemical and physical characters and intrinsic properties of porous nanostructures, herein functionalized Si porous nanowires have been prepared and employed to modify electrochemical electrode for the determination of typical heavy metal ions of Pb(II) and Cd(II). First, Si nanowires have been fabricated with numerous meso-porous structures through an Ag-assisted chemical etching approach. After modified by MPTMS and APTES, thiol and amino groups are grafted on the surface of porous Si nanowires and even on the interior wall of porous holes. Then, their electrochemical sensing performances toward Pb(II) and Cd (II) have been evaluated. The results indicate that high sensitivities have been achieved owing to the strong complexing capacity of thiol and amino groups to Cd(II) and Pb(II). Notably, porous Si nanowires as promising carriers can be easily modified with other functional groups owing to their surface activity. So this approach can be further extended to selectively detect other heavy metal ions through modifying porous Si nanowires with specific organic groups.

2. Experimental Details

2.1. Chemicals and Reagents

All chemicals and reagents were purchased from Aldrich and used as received without further purification. Milli-Q water with a resistivity of greater than 18.0 MΩ·cm was used in the preparation of aqueous solutions.

2.2. Preparation of thiol and amino-functionalized porous Si nanowires

To prepare Si nanowires with meso-porous structures, heavily ($< 0.005\ \Omega$ cm) doped p-type Si (100) wafers were employed and etched via an Ag-assisted chemical etching approach similar with previous reports [26]. Differently, the etching time increased to 30 min in order to increase the length of Si nanowires. After completely removing the catalyst of Ag, their modifications were performed. First, as-prepared porous Si nanowires scratched from the silicon substrate were dispersed into 97% H_2SO_4/30% H_2O_2 (3:1, v/v) at 60 °C for 30 min to develop hydroxyl groups on their surfaces. After centrifugation and washing with DI water for several time, certain amount of them were added into in anhydrous toluene with excess MPTMS or APTES and refluxed for 6 h at 80 °C. Then thiol or amino-functionalized Si nanowires were obtained via centrifugation and washing with toluene, ethanol and water, respectively. Finally, all achieved samples were dried in air.

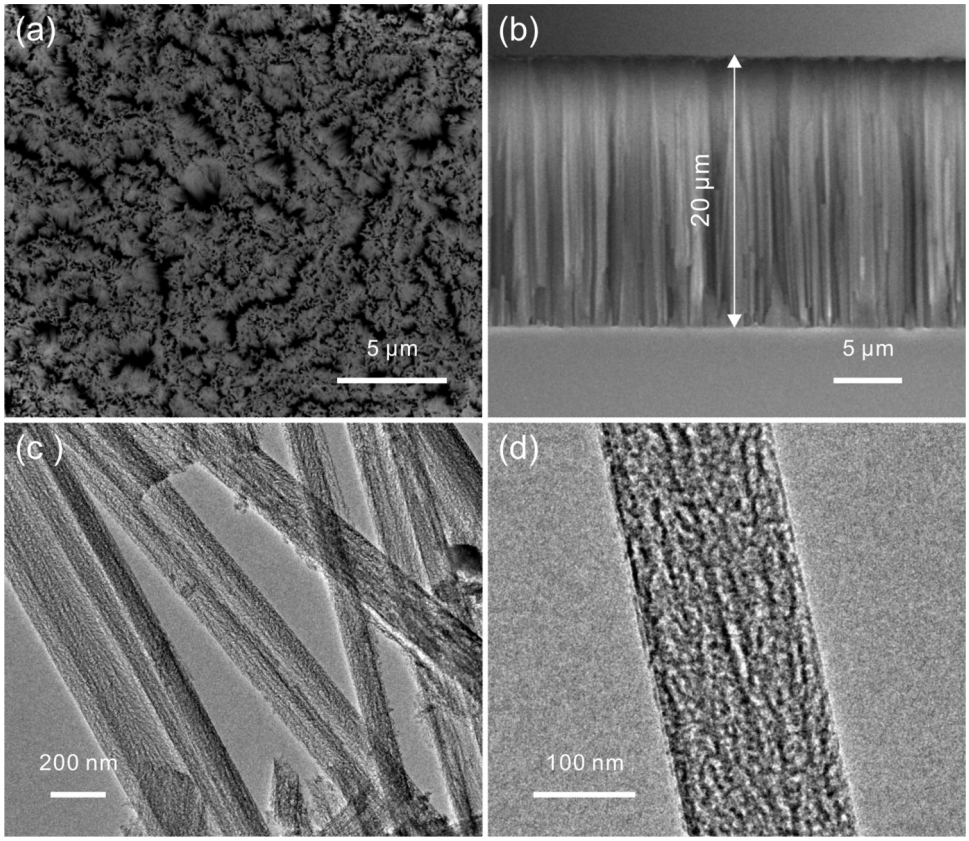

Fig 1. (a) top-view SEM image, (b) cross sectional SEM image, and (c) TEM image of as-prepared porous Si nanowires array; (d) high-magnified TEM image of individual nanowire.

2.3. Fabrication of modified electrode

Prior to modification, glassy carbon electrodes (GCE) were polished sequentially with aqueous slurries of 1 and 0.05 μm size alumina powder and sonicated for 1 min in deionized water after each stage of polishing, and then CV (Cyclic Voltammetry) characteristics was employed in 0.5 mM $K_3Fe(CN)_6$ with 0.1 M KCl solution at scan rate 50 mV s^{-1} until a quasi-reversible redox reaction was presented. The fabrication of the modified GCE was performed as follows: First, thiol or amino-functionalized porous Si nanowires (10 mg) were dissolved in 1 mL of ethanol and sonicated for 30 min to get a homogeneous suspension. Then a 5 mL of the obtained suspension was pipetted onto the freshly polished surface of GCE. After drying in the air, 2.5 μL of Nafion ethanol solution (0.5 wt. %) was dropped again on its surface to fix the modifiers. For comparison, pristine porous Si nanowires modified GCE was also prepared in the same approach.

2.4. Characterization of as-prepared samples and electrochemical measurements

The morphologies and microstructures of as-prepared samples were investigated with a Quanta 200 FEG Environmental scanning electronic microscopy (ESEM) and JEOL 2010 transmission electron microscopy (TEM). The infrared (IR) spectra were obtained with a Nicolet Nexus-670 FT-IR spectrometer. X-Ray photoelectron spectroscopy (XPS) analyses of the samples were conducted on a VG ESCALAB MKII spectrometer using an Mg Kα X-ray source (1253.6 eV, 120 W) at a constant analyzer. The energy scale was internally calibrated by referencing the binding energy (E_b) of the C 1 s peak at 284.60 eV for contaminated carbon.

All electrochemical measurements were carried out using a computer-controlled potentiostat (CHI 621B) and preformed in a conventional three-electrode cell comprising the modified glassy carbon electrode as a working electrode, a platinum wire as a counter electrode, and an Ag/AgCl in saturated KCl solution as a reference electrode. Square wave anodic stripping voltammetry (SWASV) was used for the following detection under optimized conditions. Cd(II) and Pb(II) were reduced and accumulated at the potential of −1.2 V for 180 s in 0.1 M NaAc-HAc (pH = 4.0). Subsequent anodic stripping was performed in the potential range of −1.2 to 0.4 V with a step potential of 4 mV, frequency of 15 Hz and amplitude of 25 mV. The simultaneous and selective detection of Cd(II) and Pb(II) has been performed under the same experimental conditions. All electrochemical data were subjected to statistical analysis and were presented with error bars corresponding to standard errors after repeatedly measured for 5 times.

3. Results and discussion

3.1. Fabrication of porous Si nanowires and their functionization

Via a typical Ag-assisted chemical etching approach, porous Si nanowires have been fabricated, which is similar to our previous report [26]. As shown in Fig. 1**a**, as-prepared Si nanowires array is high density and large scale. After etching for around 30 min, the length of Si nanowires is up to about 20 μm from their cross-sectional view, displayed in Fig. 1**b**. In Fig. 1**c**, TEM images of the fabricated nanowires are presented. Evidently, as-prepared nanowires are uniformly and highly porous nanostructure. From highly magnified TEM image shown in Fig. 1**d**, it can be further confirmed that it belongs to meso-porous structure. Accordingly, as-prepared porous Si nanowires are endowed with higher surface area in contrast to their solid one, leading to a widely potential application.

To enhance the absorption of porous Si nanowires toward to specific heavy metal ion, thiol(–SH) and amino(–NH_2) functionization have been further performed. Their schematic processes are presented in Fig. 2**a**, analogous to previous reports [33,34]. In Fig. 2**b**, FT-IR spectrums of pristine, amino- and thiol-porous Si nanowires are presented. For pristine porous Si nanowires (Si NWs), the vibrating bands in the range of 1100–800 cm^{-1} are attributed to the asymmetric and symmetric stretching modes of Si–O groups arising from the thin layer of SiO_2 formed on their surfaces. After anchoring MPTMS and APTES onto porous Si

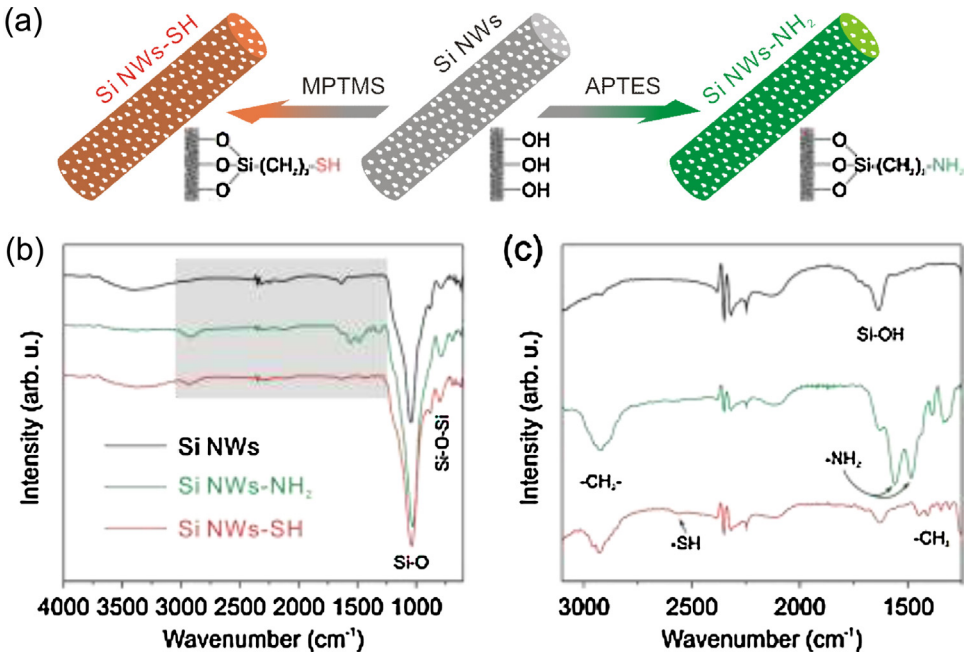

Fig. 2. (a) schematic process of thiol (—SH) and amino(—NH_2) functionization of porous Si nanowires; (b) FTIR spectra of pristine porous Si nanowires(Si NWs), amino-functionalized porous Si nanowires(Si NWs-NH_2), and thiol-functionalized porous Si nanowires(Si NWs-SH); (c) FTIR spectra corresponding to the magnified spectra ranging from 1250 to 3100 cm^{-1} of Si NWs, Si NWs-NH_2, and Si NWs-SH.

nanowires, two bands in the range of 2950–2850 cm^{-1} are emerged, which is ascribed to the vibrating bands of —CH_2–. For the amino-Si nanowires (Si NWs-NH_2), two new major peaks centered at about 1484 and 1559 cm^{-1} are emerged, which are ascribed to the asymmetric and symmetric stretching vibrations of the —NH_2 groups, respectively. For the thiol-Si nanowires (Si NWs-SH), it could be easily observed that the characteristic vibration peak corresponding to –SH is emerged at about 2556 cm^{-1} although it is very weak. Based on the above results, it can be clearly concluded that porous Si nanowires are successfully grafted with functional groups of —NH_2 and —SH after modified by APTES and MPTMS, respectively.

From their X-ray photoelectron spectra (XPS), the above results can be further confirmed. As shown in Fig. 3**a**, a strong oxygen peak besides the peaks of Si is appeared for the pristine porous Si nanowires due to the formation of a very thin shell of SiO_2 in air. The F peak arises from the residual of HF during the etched process. Notably, the weak C peak is from the carbon dioxide in air or organic remnants during the fabrication process. After modification with APTES, the intensity of C peak is greatly increased, as displayed in Fig. 3**b**. Additionally, the N peak is emerged, indicating that porous Si nanowires are modified by numerous —NH_2 groups. In Fig. 3**c**, the emergences of S peaks confirm that –SH groups are exposed on the porous Si nanowires after thiol-modification. Moreover, the intensity of C peak is also increased, similar with amino-porous Si nanowires.

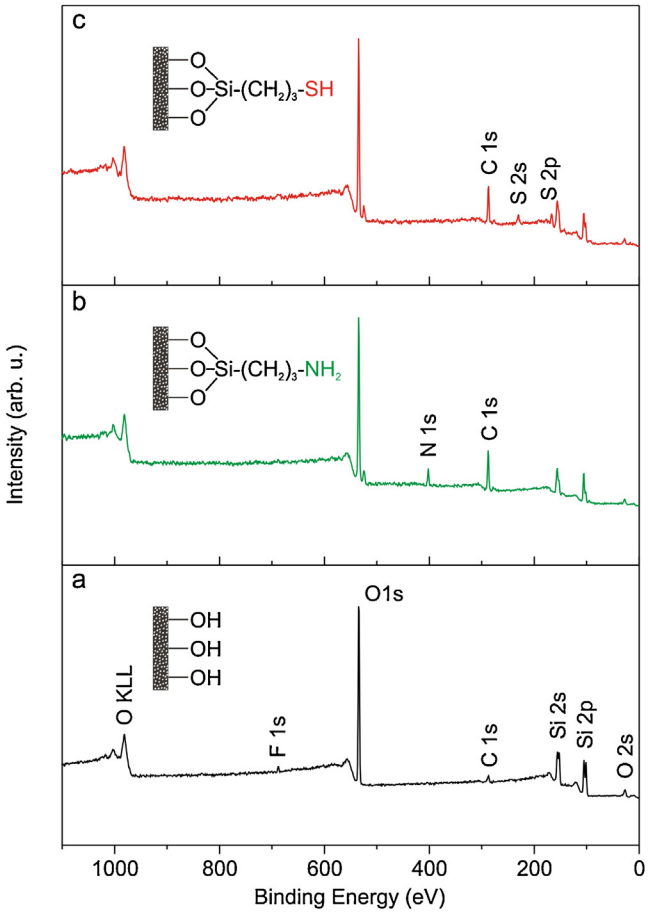

Fig. 3. XPS spectra of (a) pristine porous Si nanowires, (b) amino-functionalized porous Si nanowires, and (c) thiol-functionalized porous Si nanowires.

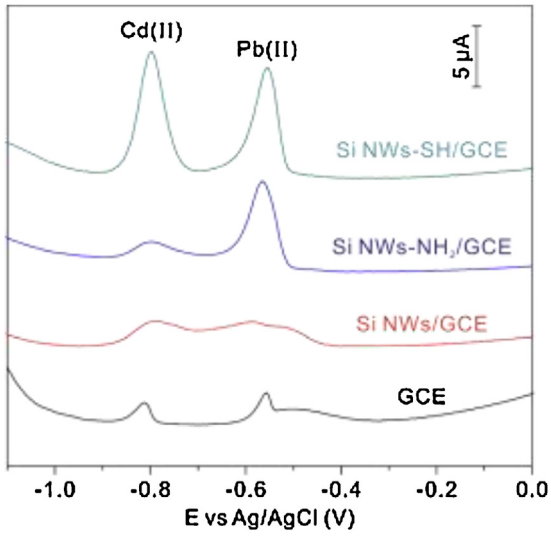

Fig. 4. SWASV curves of bare GCE, Si NWs/GCE, Si NWs-NH_2/GCE, and Si NWs-SH/GCE to 500 nM Cd(II) and 250 nM Pb(II) at the accumulation potential of –1.2 V with accumulation time of 180 s in HAc-NaAc (pH = 4.0).

3.2. Enhanced electrochemical sensing behaviors of functional porous Si nanowires(Si NWs) toward Cd(II) and Pb(II)

In order to demonstrate the enhanced effects of electrochemical sensing behaviors towards heavy metal ions, SWASV curves of different modified electrodes have been performed, as shown in Fig. 4. Under a typical electrochemical detecting conditions, we can observe that the striping peaks of Cd(II) and Pb(II) is still weak on pristine porous Si nanowires modified GCE (Si NWs/GCE), compared with those on bare GCE. For amino-porous Si nanowires modified GCE (Si NWs-NH_2/GCE), the striping peak of Pb(II) greatly increases. Meanwhile, it cannot improve the stripping behavior to Cd(II). This result is arised from the strong complexing interaction between —NH_2 and Pb(II) [35]. Notably, for the thiol-porous Si nanowires modified GCE (Si NWs-SH/GCE), their stripping behaviors for Cd(II) and Pb(II) are both greatly enhanced. It is well agreement with previous reports that thiol functional groups present a good absorbing performance toward Cd(II) and Pb(II), enhancing their electrochemical responses [36–38]. These results suggest that the Si NWs modified with different functional groups exhibit different stripping behaviors toward different heavy metal ions.

3.3. Optimization of experimental conditions

For the stripping behaviors of heavy metal ions on electrochemical electrode, it usually affected by pH value of supporting electrolyte solution, accumulation time and potential. To obtain the optimal above parameters, Si NWs-SH/GCE toward Cd(II) as an example was employed. Based on SWASV curves shown in Fig. 5**a**, the strength of stripping peaks is evidently affected by pH value. At about pH 4.0, it presents the strongest stripping peaks, as shown in Fig. 5**b**. Therefore, the supporting electrolyte of pH 4.0 is employed in the following detection. Besides its strength, the potential of stripping peak weakly and positively shifted with the increase of pH value.

Moreover, the accumulation time can affect the amount of analyte accumulated onto electrode surface, which further affects the detection limit and the sensitivity. So the dependence of peak currents on the accumulation time has been also studied and the results are depicted in Fig. 5**c**. Clearly, the response of the stripping peak currents of Cd(II) is enhanced with the increase of the

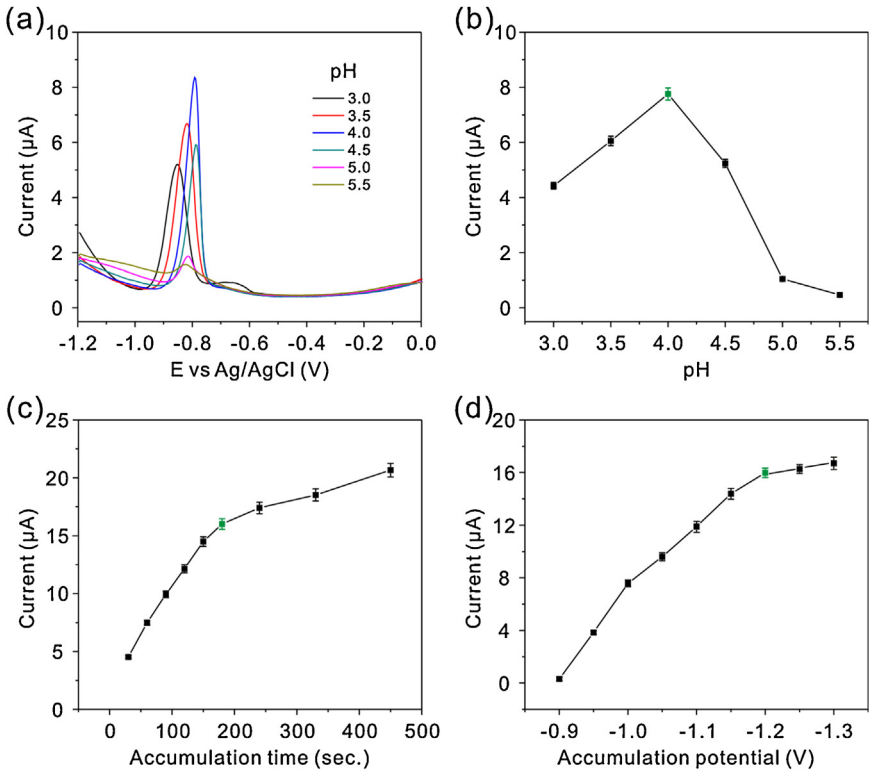

Fig. 5. (a) SWASV curves for Si NWs-SH/GCE to 200 nM Cd(II) in 0.1 M HAc-NaAc buffer solution with different pH value for accumulation time of 180 s at accumulation potential of −1.2 V and (b) the corresponding plot of stripping peak current *versus* pH value; (c) the plot of stripping peak current *versus* accumulation time to 500 nM Cd(II) in 0.1 M HAc-NaAc (pH = 4.0) buffer solution at accumulation potential of −1.2 V, and (d) the plot of stripping peak current *versus* accumulation potential to 500 nM Cd(II) in 0.1 M HAc-NaAc (pH = 4.0) buffer solution for accumulation time of 180 s.

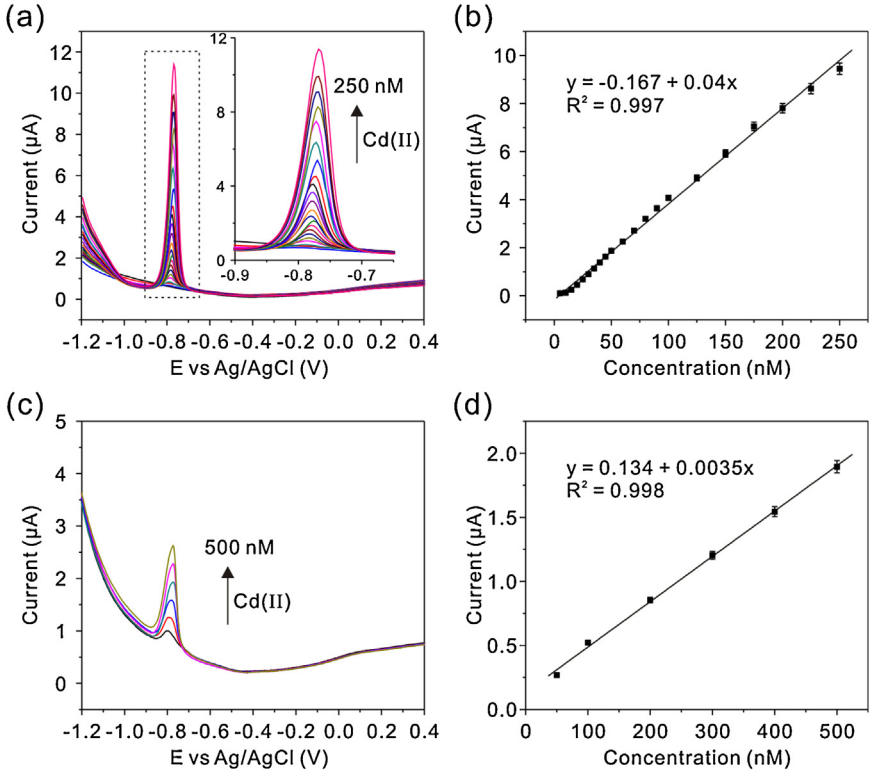

Fig. 6. SWASV curves of (a) Si NWs-SH/GCE and (c) Si NWs-NH_2/GCE to different concentration of Cd(II); The relationship between concentration and stripping current for (b) Si NWs-SH/GCE and (d) Si NWs-NH_2/GCE at the accumulation potential of −1.2 V with the accumulation time of 180 s in HAc-NaAc (pH = 4.0).

accumulation time and reached a slower growth at 180 s. It is due to the increased amount of analyte on the modified electrode surface and subsequently become saturated. Although increasing the accumulation time improves the sensitivity, it also lowers the upper detection limit due to the surface saturation at high metal ions concentrations [39]. Therefore, to achieve lower detection limit and wider response range, the accumulation time of 180 s was chosen for further detection.

In stripping analysis, the application of adequate accumulation potential is also very important to achieve the best sensitivity. Thus the effect of the accumulation potential on the peak current after 180 s accumulation was studied in the potential range from −0.9 V to −1.3 V. As shown in Fig. 5**d**, the resulting stripping current increases when the accumulation potential shifts from −0.9 V to −1.2 V and reached a plateau after −1.2 V. Thus, we choose −1.2 V as the optimal accumulation potential for the subsequent stripping experiment.

3.4. Detection of Pb(II) and Cd(II)

First, striping behaviors of Cd(II) has been investigated at Si NWs-SH/GCE and Si NWs-NH_2/GCE, respectively. SWASV curves for Si NWs-SH/GCE toward different concentrations of Cd(II) are shown in Fig. 6**a**. It can be found that the stripping currents increase with the increase of the concentrations of Cd(II). According to the relationship between stripping current and concentration, a well-defined linear curve has been presented in the range from 5 to 250 nM. Compared with Si NWs-SH/GCE, the response toward Cd(II) is weaker for Si NWs-NH_2/GCE. Fig. 6**c** shows the stripping curves of different concentration of Cd(II) at Si NWs-NH_2/GCE. Clearly the stripping current is lower than that on Si NWs-SH/GCE under the same concentration of Cd(II). From the relationship between stripping current and concentration of Cd(II) shown in Fig. 6**d**, obviously the sensitivity of Si NWs-NH_2/GCE (0.0035 μA/nM) is also lower than that on Si NWs-SH/GCE (0.04 μA/nM) given in Fig. 6**b**. This difference may be due to that thiol-function Si NWs present a higher affinity than that of amino-function Si NWs.

In addition, the responses of the modified electrodes towards Pb(II) have also been performed. For Si NWs-SH/GCE, the stripping currents at −0.55 V greatly increase with the concentration of Pb (II) (Fig. 7**a**). Similar result is also obtained for Si NWs-NH_2/GCE (Fig. 7**c**). In contrast with Cd(II), Si NWs-SH/GCE and Si NWs-NH_2/GCE both show a better preconcentration toward Pb(II). However, Si NWs-SH/GCE still present a better response to Pb(II) than that of Si NWs-NH_2/GCE, which can be inferred from their relationships between stripping current and concentration of Pb(II) shown in Fig. 7**b** and **d**. The sensitivity of Si NWs-NH_2/GCE toward Pb(II) (0.036 μA/nM) is also lower than that on Si NWs-SH/GCE (0.074 μA/nM).

Simultaneous measurement of Cd(II) and Pb(II) was also performed, as shown in Fig. 8**a**, it can be seen that Si NWs-SH/GCE shows individual peaks at about −0.6 and −0.8 V for Pb(II) and Cd(II) in their coexistence. Linear increase in the stripping peak current is achieved with the increase of the concentration of Pb(II) and Cd(II) simultaneously. Notably, the sensitivity of the electrode almost does not change when these two ions coexist at the concentration tested in this investigation (Fig. 8**b**). The sensitivities for individual and simultaneous measurements of Cd(II) and Pb(II) are comparable, indicating that simultaneous measurement of Cd (II) and Pb(II) on Si NWs-SH/GCE is feasible. For Si NWs-NH_2/GCE, it can realize selective detection of Pb(II) due to the weak response toward Cd(II) (0.036 μA/nM vs. 0.0035 μA/nM).

After finishing the individual and simultaneous measurements of Pb(II) and Cd(II), we next seek to investigate the mutual interferences between Pb(II) and Cd(II) at the Si NWs-SH/GCE.

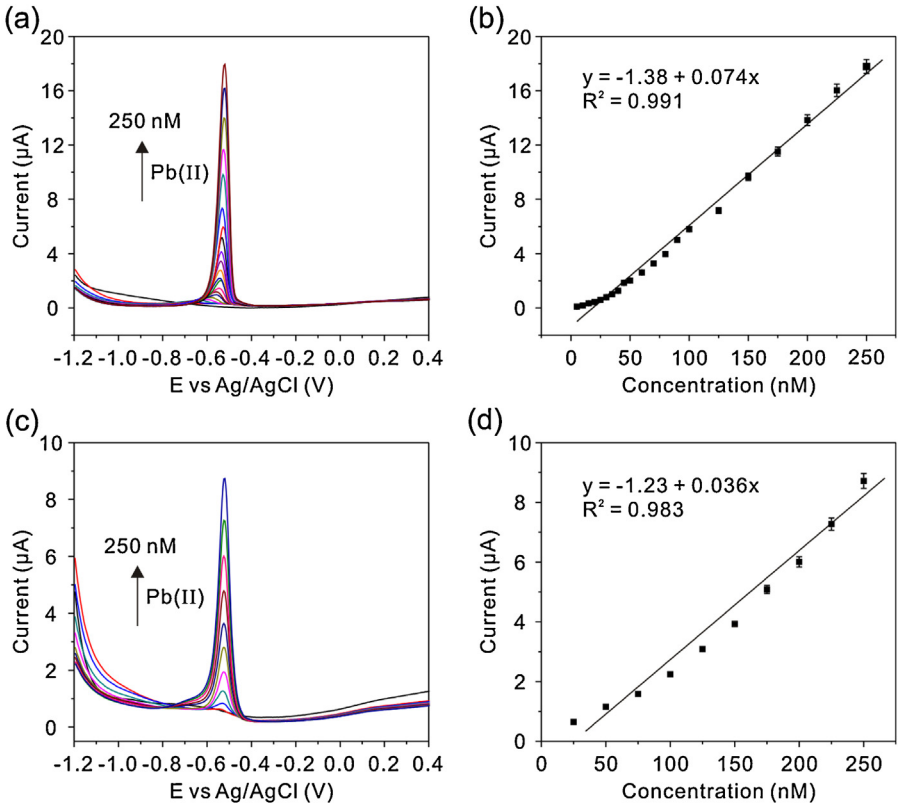

Fig. 7. SWASV curves of (a) Si NWs-SH/GCE and (c) Si NWs-NH_2/GCE to different concentration of Pb(II); The relationship between concentration and stripping peak current for (b) Si NWs-SH/GCE and (d) Si NWs-NH_2/GCE at the accumulation potential of −1.2 V with the accumulation time of 180 s in HAc-NaAc (pH = 4.0).

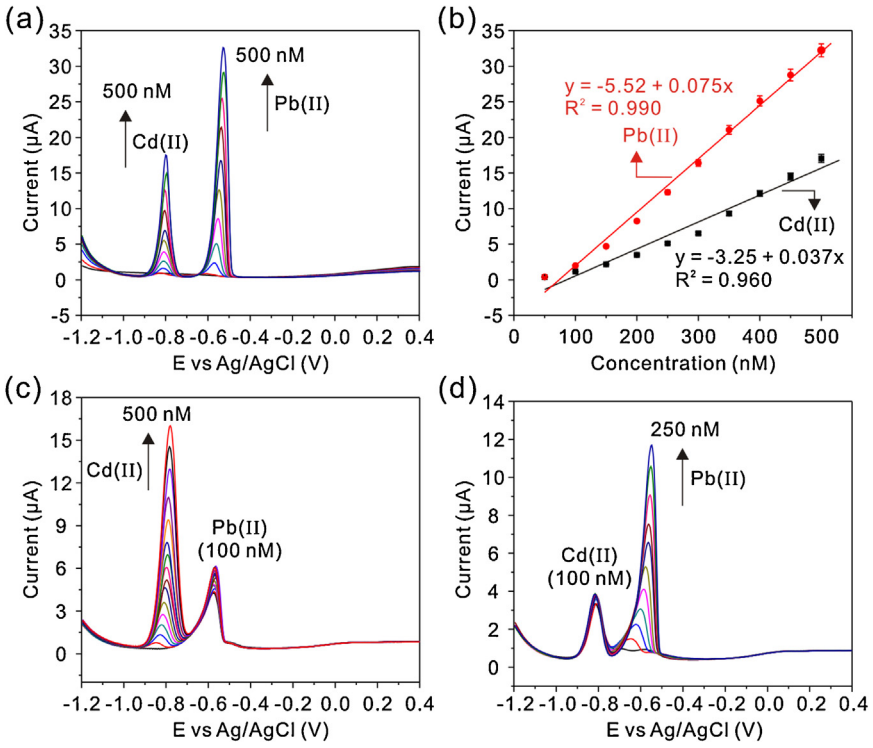

Fig. 8. (a) SWASV curves and (b) the relationship between concentration and stripping current of the simultaneous detection of Pb(II) and Cd(II) for Si NWs-SH/GCE; SWASV curves of Si NWs-SH/GCE: (c) for different concentration of Cd(II) in the presence of 100 nM Pb(II); (d) for different concentration of Pb(II) in the presence of 100 nM Cd(II). Data were recorded at the accumulation potential of −1.2 V with the accumulation time of 180 s in HAc-NaAc (pH = 4.0).

Increasing the concentration of Cd(II) in the presence of 100 nM Pb (II) (Fig. 8**c**), the stripping peak current for Cd(II) also gradually increases. Simultaneously, the stripping curves for Pb(II) is fundamentally remained. Moreover, the peak for Cd(II) can be still linearly increased and the sensitivity is very close to that for individual measurement. Similar phenomenon could be observed for different concentration of Pb(II) in the presence of 100 nM Cd (II), as shown in Fig. 8**d**. All the results indicate that the electrochemical response of Pb(II) or Cd(II) on the Si NWs-SH/GCE is unaffected by the presence of another ion.

3.5. Selectivity

The selectivity of the Si NWs-SH/GCE and Si NWs-NH_2/GCE are determined by challenging it with several heavy metal ions. Typical heavy metal ions including Cu(II), Zn(II) and Cr(III) are chosen as potential interfering ions for investigating their selectivity. Experiments were performed individually in 0.1 M NaAc-HAc (pH 4.0) containing each single metal ion. The results are shown in Fig. 9. In the potential range of −1.2 to 0.4 V, little stripping peak current signal could be observed for each metal ion mentioned above, even though they are at the high concentrations of 5 μM compared with that of pure 250 nM Pb(II) and Cd(II). The results suggest that the potential interfering ions have no significant influences on the stripping peak current of Cd(II) and Pb(II).

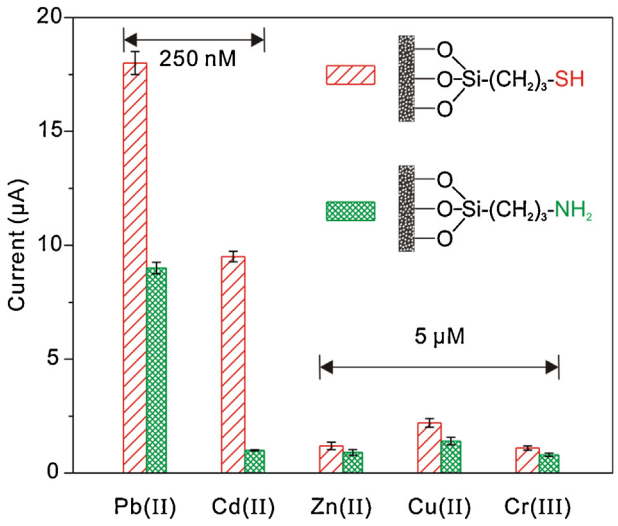

Fig. 9. Selectivity studies of Si NWs-SH/GCE and Si NWs-NH_2/GCE. Data were recorded at the accumulation potential of −1.2 V with the accumulation time of 180 s in HAc-NaAc (pH = 4.0).

4. Conclusion

In summary, thiol and amino-functionalized Si porous nanowires have been successfully prepared via a chemical modification with MPTMS and APTES, respectively. Electrochemical results demonstrate that they can be employed to modify electrodes to selectively detect Cd(II) and Pb(II) with high sensitivity, which is ascribed to the strong complexing capacity of thiol and amino groups. Furthermore, porous Si nanowires decorated with thiol groups present different stripping behaviors from those with amino groups toward Cd(II) and Pb(II). They both show better sensing performances toward Pb(II) in contrast to Cd(II). But thiol-functionalized Si porous nanowires present higher sensitivity with 0.04 μA/nM and 0.074 μA/nM toward Cd(II) and Pb(II), respectively. Moreover, simultaneous detection of Cd(II) and Pb(II) has also been demonstrated without any interference. Their sensing performances are not affected by other metal ions, fundamentally

preserving their individual high sensitivity. We believe that porous Si nanowires can be expectedly used as an effective modifier to selectively detect other heavy metal ions through modifying with other specific organic groups.

Acknowledgments

This work was supported by the National Natural Science Foundation of China (Grant No. 61474122, 21475133 and U1532123), the National Key Scientific Program-Nanoscience and Nanotechnology (2013CB934300), and Brain Korea 21 project, School of Electrical Engineering, Korea Advanced Institute of Science and Technology in 2011.

References

[1] A.K. Wanekaya, Applications of nanoscale carbon-based materials in heavy metal sensing and detection, Analyst 136 (2011) 4383–4391.
[2] H.N. Kim, W.X. Ren, J.S. Kim, J. Yoon, Fluorescent and colorimetric sensors for detection of lead cadmium, and mercury ions, Chem. Soc. Rev. 41 (2012) 3210–3244.
[3] Y.-W. Lin, C.-C. Huang, H.-T. Chang, Gold nanoparticle probes for the detection of mercury, lead and copper ions, Analyst 136 (2011) 863–871.
[4] G. Aragay, J. Pons, A. Merkoçi, Recent trends in macro- micro-, and nanomaterial-based tools and strategies for heavy-metal detection, Chem. Rev. 111 (2011) 3433–3458.
[5] M. Li, H.L. Gou, I. Al-Ogaidi, N.Q. Wu, Nanostructured sensors for detection of heavy metals: a review, ACS Sustain Chem. Eng. 1 (2013) 713–723.
[6] G. Herzog, V. Beni, Stripping voltammetry at micro-interface arrays: a review, Anal. Chim. Acta 769 (2013) 10–21.
[7] D.E. Mays, A. Hussam, Voltammetric methods for determination and speciation of inorganic arsenic in the environment—a review, Anal. Chim. Acta 646 (2009) 6–16.
[8] R.J.C. Brown, M.J.T. Milton, Analytical techniques for trace element analysis: an overview, TrAC-Trend. Anal. Chem. 24 (2005) 266–274.
[9] K.A. Howell, E.P. Achterberg, C.B. Braungardt, A.D. Tappin, P.J. Worsfold, D.R. Turner, Voltammetric in situ measurements of trace metals in coastal waters, TrAC-Trend. Anal. Chem. 22 (2003) 828–835.
[10] J.M. Gong, T. Zhou, D.D. Song, L.Z. Zhang, X.L. Hu, Stripping voltammetric detection of mercury(II) based on a bimetallic Au-Pt inorganic-organic hybrid nanocomposite modified glassy carbon electrode, Anal. Chem. 82 (2010) 567–573.
[11] C. Gao, X.-J. Huang, Voltammetric determination of mercury(II), TrAC-Trend. Anal. Chem. 51 (2013) 1–12.
[12] Z.-G. Liu, X.-J. Huang, Voltammetric determination of inorganic arsenic, TrAC-Trend. Anal. Chem. 60 (2014) 25–35.
[13] J.T. Zhang, Z.Y. Jin, W.C. Li, W. Dong, A.H. Lu, Graphene modified carbon nanosheets for electrochemical detection of Pb(II) in water, J. Mater. Chem. A 1 (2013) 13139–13145.
[14] G. Aragay, J. Pons, A. Merkoci, Recent trends in macro- micro-, and nanomaterial-based tools and strategies for heavy-metal detection, Chem. Rev. 111 (2011) 3433–3458.
[15] Z. Guo, Y. Wei, R. Yang, J.H. Liu, X.J. Huang, Hydroxylation/carbonylation carbonaceous microspheres: A route without the need for an external functionalization to a hunter of lead(II) for electrochemical detection, Electrochim. Acta 87 (2013) 46–52.
[16] Y. Wei, R. Yang, Y.X. Zhang, L. Wang, J.H. Liu, X.J. Huang, High adsorptive gamma-AlOOH(boehmite)@SiO_2/Fe_3O_4 porous magnetic microspheres for detection of toxic metal ions in drinking water, Chem. Commun. 47 (2011) 11062–11064.
[17] S.Z. Kang, Z.Y. Cui, J. Mu, High sensitivity to Cu^{2+} ions of electrodes coated with ethylenediamine-modified multi-walled carbon nanotubes, Nanotechnology 17 (2006) 4825–4829.
[18] J. Morton, N. Havens, A. Mugweru, A.K. Wanekaya, Detection of trace heavy metal ions using carbon nanotube-modified electrodes, Electroanalysis 21 (2009) 1597–1603.
[19] X.C. Fu, J. Wu, L. Nie, C.G. Xie, J.H. Liu, X.J. Huang, Electropolymerized surface ion imprinting films on a gold nanoparticles/single-wall carbon nanotube nanohybrids modified glassy carbon electrode for electrochemical detection of trace mercury(II) in water, Anal. Chim. Acta 720 (2012) 29–37.
[20] Z.Q. Zhao, X. Chen, Q. Yang, J.H. Liu, X.J. Huang, Selective adsorption toward toxic metal ions results in selective response: electrochemical studies on a polypyrrole/reduced graphene oxide nanocomposite, Chem. Commun. 48 (2012) 2180–2182.
[21] S.J. Wu, F.T. Li, R. Xu, S.H. Wei, G.T. Li, Synthesis of thiol-functionalized MCM-41 mesoporous silicas and its application in Cu(II), Pb(II) Ag(I), and Cr(III) removal, J. Nanopart. Res. 12 (2010) 2111–2124.
[22] B. Lee, Y. Kim, H. Lee, J. Yi, Synthesis of functionalized porous silicas via templating method as heavy metal ion adsorbents: the introduction of surface hydrophilicity onto the surface of adsorbents, Micropor. Mesopor. Mat. 50 (2001) 77–90.
[23] A. Bibby, L. Mercier, Mercury(II) ion adsorption behavior in thiol-functionalized mesoporous silica microspheres, Chem. Mater. 14 (2002) 1591–1597.
[24] T.M. Abdel-Fattah, S.M.S. Haggag, M.E. Mahmoud, Heavy metal ions extraction from aqueous media using nanoporous silica, Chem. Eng. J. 175 (2011) 117–123.
[25] A. Walcarius, C. Delacote, Mercury(II) binding to thiol-functionalized mesoporous silicas: critical effect of pH and sorbent properties on capacity and selectivity, Anal. Chim. Acta 547 (2005) 3–13.
[26] Z. Guo, M.L. Seol, M.S. Kim, J.H. Ahn, Y.K. Choi, J.H. Liu, X.J. Huang, Hollow CuO nanospheres uniformly anchored on porous Si nanowires: preparation and their potential use as electrochemical sensors, Nanoscale 4 (2012) 7525–7531.
[27] J.F. Huang, Y.H. Zhu, H. Zhong, X.L. Yang, C.Z. Li, Dispersed CuO nanoparticles on a silicon nanowire for improved performance of nonenzymatic H_2O_2 detection, ACS Appl. Mater. Inter. 6 (2014) 7055–7062.
[28] Z.N. Liu, B.L. Yadian, H. Liu, C. Liu, B.W. Zhang, R.V. Ramanujan, Y.Z. Huang, Fabrication of hybrid CuO/Pt/Si nanoarray for non-enzymatic glucose sensing, Electrochem. Commun. 33 (2013) 138–141.
[29] W. Yantasee, B. Charnhattakorn, G.E. Fryxell, Y.H. Lin, C. Timchalk, R.S. Addleman, Detection of Cd, Pb, and Cu in non-pretreated natural waters and urine with thiol functionalized mesoporous silica and Nafion composite electrodes, Anal. Chim. Acta 620 (2008) 55–63.
[30] D.E. Popa, M. Buleandra, M. Mureseanu, M. Ionica, I.G. Tanase, Organofunctionalized mesoporous silica carbon paste electrode for voltammetric determination of Pb(II), Rev. Roum. Chim. 55 (2010) 565-.
[31] D.E. Popa, M. Buleandra, M. Mureseanu, M. Ionica, I.G. Tanase, Carbon paste electrode modified with organofunctionalized mesoporous silica for electrochemical detection and quantitative determination of cadmium (II) using square wave anodic stripping voltammetry, Rev. Chim-Bucharest 61 (2010) 162–167.
[32] D.E. Popa, M. Mureseanu, I.G. Tanase, Organofunctionalized mesoporous silica carbon paste electrode for simultaneously determination of copper, lead and cadmium, Rev. Chim-Bucharest 63 (2012) 507–512.
[33] T. Suteewong, H. Sai, M. Bradbury, L.A. Estroff, S.M. Gruner, U. Wiesner, Synthesis and formation mechanism of aminated mesoporous silica nanoparticles, Chem. Mater. 24 (2012) 3895–3905.
[34] Y.F. Shen, T. Wu, Y.J. Zhang, J.H. Li, Comparison of two-typed (3-mercaptopropyl)trimethoxysilane-based networks on Au substrates, Talanta 65 (2005) 481–488.
[35] A.M. Showkat, Y.P. Zhang, M.S. Kim, A.I. Gopalan, K.R. Reddy, K.P. Lee, Analysis of heavy metal toxic ions by adsorption onto amino-functionalized ordered mesoporous silica, Bull. Korean Chem. Soc. 28 (2007) 1985–1992.
[36] J. Guo, Y.P. Luo, F. Ge, Y.L. Ding, J.J. Fei, Voltammetric determination of cadmium (II) based on a composite film of a thiol-functionalized mesoporous molecular sieve and an ionic liquid, Microchim. Acta 172 (2011) 387–393.
[37] W. Yantasee, C.L. Warner, T. Sangvanich, R.S. Addleman, T.G. Carter, R.J. Wiacek, G.E. Fryxell, C. Timchalk, M.G. Warner, Removal of heavy metals from aqueous systems with thiol functionalized superparamagnetic nanoparticles, Environ. Sci. Technol. 41 (2007) 5114–5119.
[38] N. Zhang, B. Hu, Cadmium (II) imprinted 3-mercaptopropyltrimethoxysilane coated stir bar for selective extraction of trace cadmium from environmental water samples followed by inductively coupled plasma mass spectrometry detection, Anal. Chim. Acta 723 (2012) 54–60.
[39] X.H. Gao, W.Z. Wei, L. Yang, M.L. Guo, Carbon nanotubes/poly(1,2-diaminobenzene) nanoporous composite film electrode prepared by multipulse potentiostatic electropolymerisation and its application to determination of trace heavy metal ions, Electroanalysis 18 (2006) 485–492.